Hindawi
Journal of Nanomaterials
Volume 2022, Article ID 7816372, 10 pages
https://doi.org/10.1155/2022/7816372

Research Article

Wear Behavioral Study of Hexagonal Boron Nitride and Cubic Boron Nitride-Reinforced Aluminum MMC with Sample Analysis

Vasudeva Rao,[1] P. Periyaswamy,[1] A. Bovas Herbert Bejaxhin,[2] E. Naveen,[3] N. Ramanan,[4] and Aklilu Teklemariam[5]

[1]*Department of Mechanical Engineering, St. Peter's Institute of Higher Education and Research, Avadi, Chennai, India*
[2]*Institute of Mechanical Engineering, Saveetha School of Engineering, SIMATS, Thandalam, Chennai, India*
[3]*Department of Mechanical Engineering, Sri Sairam Engineering College, Chennai, India*
[4]*Department of Research & Development, Sync Engineering, Ambattur I.E. Ambattur, Chennai, India*
[5]*Department of Mechanical Engineering, Faculty of Manufacturing, Institute of Technology, Hawassa University, Ethiopia*

Correspondence should be addressed to A. Bovas Herbert Bejaxhin; herbert.mech2007@gmail.com
and Aklilu Teklemariam; akliluteklemariam@hu.edu.et

Received 8 February 2022; Accepted 12 April 2022; Published 24 May 2022

Academic Editor: Chang Chuan Lee

During the stir casting process, different percent weights of hexagonal boron nitride (HBN) and cubic boron nitride (CBN) were mixed with aluminum alloy 6061. The test specimens are then machined from the cast aluminum metal matrix composites. The tests are carried out utilizing an ASTM G99-compliant pin-on-plate tribometer on a pivoting EN32 circle. Minitab 16 is used to plan the dry sliding wear trials, which are set up in an orthogonal array. The input parameters are percent HBN addition and CBN addition, sliding speed, and load, and the wear rate was considered to be the output parameter. The actual density of the cast specimens was found to be greater than 90% of their theoretical density. The accumulation of HBN and CBN greatly enhances the wear resistance of aluminum metal matrix composites, according to research. The technique of regression analysis is utilized to establish genuine links between the wear rate and input parameters. The morphology of the worn out surfaces was examined using a scanning electron microscope (SEM). After numerous iterations, the simulation source of DEFORM 3D forecasts the stress and velocity component of the frictional surface contact area.

1. Introduction

The current requirement of automotive industries to improve the fuel efficiency with improved properties like friction and wear resistance that led to the development of low-+cost and lightweight materials such as cylinder blocks, liners, piston, cam shafts, lifters, and brake drum materials. Selection of the right material for an engineering application depends on properties such as strength, density, light weight, melting point, conductivity, and cost. The density of aluminum being one-third of the steel makes it still a better choice for high-strength and low-weight requirements. Though aluminum and its alloys represent better mechanical properties, it shows degradation of wear resistance, which limits its application in engineering. In order to overcome these limitations, addition of hard material (reinforcement) into soft (matrix) material improves the mechanical and tribological properties, termed as metal matrix composites (MMC).

In reference [1], AZ31B is selected as Mg matrix material and hard tungsten carbide (WC) particles as reinforcement material. Mg/WC composites reinforced with different weight proportions (0, 5, 10, and 15 wt.%) were made through the stir casting method. The wear test results denoted that the AZ31B/15 wt% WC composites have excellent tribological behavior when compared to the base magnesium matrix AZ31B alloy.

Natarajan et al. [1] evaluated the metal matrix composites (MMCs) reinforced with SiC particles that combine the matrix properties with those of the ceramic reinforcement, leading to higher stiffness and superior thermal stability with respect to the corresponding unreinforced alloys. However,

The SEM analysis of the weld zone shows evidence of a substantial grain refinement of the aluminium matrix and fracturing of reinforcement particles due to uniform distribution and dynamic recrystallization induced by the plastic deformation and frictional heating during welding.

The light-weight matrix materials used are aluminum, magnesium, and titanium. Among them, aluminum and magnesium draw the attention as preferred matrix materials due to their several attractive properties. Aluminum metal matrix composites (AMMCs) have demonstrated higher strength at high temperatures, a low coefficient of friction, thermal expansion, superior wear resistance, and stiffness. The hardness of the AMC increases with decreasing density with increasing wt percent of reinforcements. AMMCs have found its application in aircraft, aerospace, automobiles, and various other fields. The commercial application for Toyota engineering in the diesel engine piston, which offers higher wear resistance and strength at high temperatures than Cast Iron.

Wear is a property of an engineering system that is influenced by factors such as load, speed, temperature, hardness, foreign material presence, and the surrounding environment. Wearing situations may produce material wear in a variety of ways. Surface damage or material removal from one or both solid surfaces in a sliding, rolling, or impact action relative to one another might be the cause. Surface interactions at asperities are the most common source of wear. The material on the contacting surface may be removed, transferred to the mating surface, or broken apart as a wear particle during relative motion. Because a material's wear resistance is linked to its microstructure, which may change throughout the wear process, the microstructure seems to be highlighted in wear research. Wear research programmes must be thoroughly structured since metal wear is impacted by a number of elements.

As a result, some of the data has been standardized to make it more helpful. In a vehicle application, Natarajan et al. [1] evaluated traditional grey cast iron and aluminum metal matrix composite for friction material. They put the disc through a wear test, using pin as the brake shoe lining material. The disc is made of A356/25SiCp, while the pins are made of grey cast iron. Optical micrographs were used to examine the worn surfaces of Al-MMC, brake discs, and cast iron, and they concluded that Al-MMC had a higher wear resistance than cast iron. Singh [2] produced aluminum hybrid composites for tribological applications using Al/SiC/Gr. According to their findings, the hybrid composite outperforms the Al alloy in terms of wear resistance. They looked at the tribological layer, which was linked to wear patterns. The tribological properties of Al-MMC were studied by Mistry and Gohli [3]. They found that as the fraction of reinforcement in the matrix was raised, tribological property performance rose proportionately. They also discovered that reinforcing particles at the micro- and nanoscales improve wear qualities. Baradeswaran and Perumal [4] investigated the effects of B4C on Al7075 composites reinforced with K2TiF6 as a flux to prevent wetness. They discovered that increasing the volume of particles increased the composite's toughness. They also discovered that adding B4C boosted ultimate tensile, flexural, and wear strength. In addition, in the microstructure, a mechanically mixed layer of iron and oxygen was discovered. With increasing B4C, the coefficient of friction dropped and was determined to be 0.32 at 10% B4C. Padmavathi and Ramakrisnan [5] used stir casting to investigate the wear and friction behavior of Al6061 with varying percentages of the multiwall carbon nanotube (MWCNT) and SiC. When comparing severe wear circumstances to mild wear conditions, it was discovered that the composite had a low wear rate and friction coefficient. There was a threshold load over which MWCNT had a negative impact on Al alloy wear resistance. The Al reinforced with SiC and MWCNT had improved dry abrasive wear resistance, according to the findings. As the percentage of MWCNT rose, the hardness increased and the specific wear rate dropped. Siddhartha et al. [6] stir cast aluminum–boron carbide MMC with a 5 wt% B4C content and an average size of 33 m. Wear tests were carried out on Taguchi's L27 orthogonal array using three parameters and three levels of condition. The input parameters were the applied load, sliding velocity, and distance. Low load (10 N), high sliding velocity (3 m/s), and distance (2000 m/s) were determined to be the best conditions for good tribological properties. The mix projecting technique was used by Siddesh et al. [7] to make AMC of Al2219 alloy supported with B4C and MoS2 particles. The density grew as the percent weight of B4C and MoS2 increased, according to the findings. In the matrix, the microstructural analysis revealed a fine dispersion of reinforcing particles. With increasing percentages of B4C and MoS2, the yield strength, yield stress, and ductility all reduced due to the formation of voids and nucleation. The composites outperformed the unreinforced Al2219 alloy in terms of wear resistance. Sharma et al. [8] used a stir casting technique to make AA6082 MMCs enhanced with graphite particles. The reinforcement was gradually increased from 0% to 12% in 3 percent increments. The micro- and macrotoughness of the composite reduced as the number of Gr particles increased.

The composite had a lower wear rate than unreinforced composites, and an ANOVA test revealed that the sliding distance was the most important element in composite wear. Riahi and Alpas [9] investigated the wear properties of hybrid A356–10% SiC–4% graphite and A356–5% Al2O3–3% graphite manufactured using stir casting processes. The creation of a tribo layer as well as an oxidized surface on both composites' contact surfaces regulated the wear rate, resulting in a mild wear regime for both composites throughout a wide range of loads and sliding speeds. Bindumadhavan et al. [10] studied the wear impact of A356/SiC dual-particle (DPS) composites (47 m and 120 m) and single-particle-sized composites (47 m). The DPS composites demonstrated increased wear resistance because the bigger SiC particles were identified to shelter the smaller ones from abrasive action by guiding the smaller particles to fulfill the wear resistant role. Hexagonal boron nitride and cubic boron nitride reinforced aluminum wear behavior were not reported in the literature survey. Praveenkumar et al. [11] have discussed that the increased WC content improves the yield strength, flexural strength, tensile strength, and microhardness of produced composites. The homogenous dispersion of WC particles throughout the Mg matrix may be seen in SEM pictures. Periyasamy et al. [12–13] have explained that due to dynamic recrystallization

generated by plastic deformation and frictional heating during welding, the microstructure analysis of the weld zone reveals significant grain refinement of the aluminium matrix and breaking of reinforcement particles. Also, determine the mechanical properties of Mg/WC composites prepared by the stir casting method. In [14, 15, 16], AA2024/Al_2O_3/SiC/Gr- and AA6061-reinforced SiC with different leaf ashes using advanced stir casting technique were discussed by Natrayan et al. on tribological behavior improvements of AA2024/Al_2O_3/SiC/Gr- and AA6061-reinforced SiC with different leaf ashes using an advanced stir casting method.

A new attempt was made to investigate the wear behavior of such composites including various percent weights of HBN and CBN. When aluminum slides across steel without any external lubrication, it adheres to the steel, resulting in a low-shear strength contact. As a result of the soft aluminum surface being ploughed by the asperities of steel and flaking of particle flakes from the transfer coating, wear debris may occur. The addition of ceramic reinforcement to the aluminum matrix decreases friction and wear. In addition, the simulation platform DEFORM 3D can be used to analyze wear behavior by providing stress and velocity components for the frictional contact region between the disc and the pin.

2. Materials and Methods

Despite the different casting fabrication methods available, stir casting is a popular fabrication and processing method because it is reasonably inexpensive and allows for the selection of materials and processing conditions. It can sustain high efficiency rates and allow for the production of exceedingly large parts. The cost of producing parts using the mix projecting approach is around one-third to one-half of the cost of producing parts using other major procedures. Costs are expected to drop to one-tenth for high-volume production as well. The distribution of the reinforcing material in the matrix alloy must be homogeneous, and the bonding strength between these two substances must be good, in order to attain optimal metal matrix composites MMC characteristics. The age of acceptable connection between molecular fortifications and fluid aluminum metal lattice during the casting process is dependent on good wetting. Acceptable wetting necessitates strong interface connections. The particles and metal matrix may establish these connections through mutual dissolution or reactivity. The design and features of the support metal interface govern the mechanical properties of MMCs in general. The movement and distribution of stress from the lattice to the support are enabled by a more solid contact, resulting in enhanced adaptability and strength. Particle dispersion in the lattice material during the soften phase of the projection cycle is influenced by mixing speed, warming temperature, mixing duration, slurry consistency, molecule wetting, mixing adequacy, and limiting gas entrapment. The stir casting procedures with the feeding arrangements of reinforcements and molten slag deposition into the mould cavity is shown in Figures 1(a)–1(c).

2.1. SEM Characterization. The form is round, and the essential characteristic of circular powder is that it has a high wear resistance and ductile property. As a result, the powder is easily spread and quickly mixed with other materials in this circular section. The nanostructure of the size is 10 microns, so the powder material is highly ductile. Figures 2 (a) and 2(b) clearly show the size and shape of the powder. The same characterization is achieved but with different magnifications.

3. Experimental Procedure

3.1. Wear Testing. Using a pin-on-disc device, the dry sliding wear behavior of aluminum/HBN/CBN was examined (DUCOMTM brand). The game plan for pin-on-plate mechanical assembly is shown in Figure 3. The steel with the category of emergency number 32 steel can be used to make the disc, and the hardness has been recorded as 65 HRC. Procedures for an arm and linked loads, in general, press the pin against the plate at a certain load. The dry sliding wear tests were performed in accordance with the ASTM G 99 standard under dry sliding conditions of temperature (300°C, RH 55 percent and 5%). Milling and polishing cylindrical pins with a diameter of 10 mm and a length of 25 mm were done using the metallographic method. The specimens were thoroughly washed with acetone before testing to remove any dirt or foreign particles. The initial and end weights of the specimen were determined with an accuracy of 0.0001 grams using the Mitutoyo electronic weighing equipment. Wear measurement is done after a wear test to quantify the quantity of materials lost (or deteriorated) (and truly after a section in help for a while). Be contingent on the cause for the experiment, the category of wear, and the number and test size instances, and the material can be degraded as loss of weight and volume or variations in straight measurement. The disc was meant to revolve beneath the pin after the example was attached in the arm. The quantity of the workpiece is measured previously, and subsequently, the test with an alphanumeric balance and the loss of weight is calculatedly aimed at each combination of contribution limitations. The maximum wear was calculated using wear track photographs and SEM images.

4. Results and Discussions

Taguchi's three-level four factors of L_{27} orthogonal array formation were used here for this research. Table 1 shows the input constraints and their levels. Table 2 shows the observations of the wear test. Minitab 16 programming was utilized to do more research.

The wear rate must be minimized when calculating the signal-to-noise ratio; the smaller the number, the better the quality features. As a result, the following equation is used to calculate the signal-to-noise ratio for mass loss: the less you have, the better. Figure 4 shows the main effect graphs of *S*/*N* ratios on the wear rate of composites.

$$\eta = -10 \times \log_{10}\left(\frac{1}{n}\sum y_i^2\right). \quad (1)$$

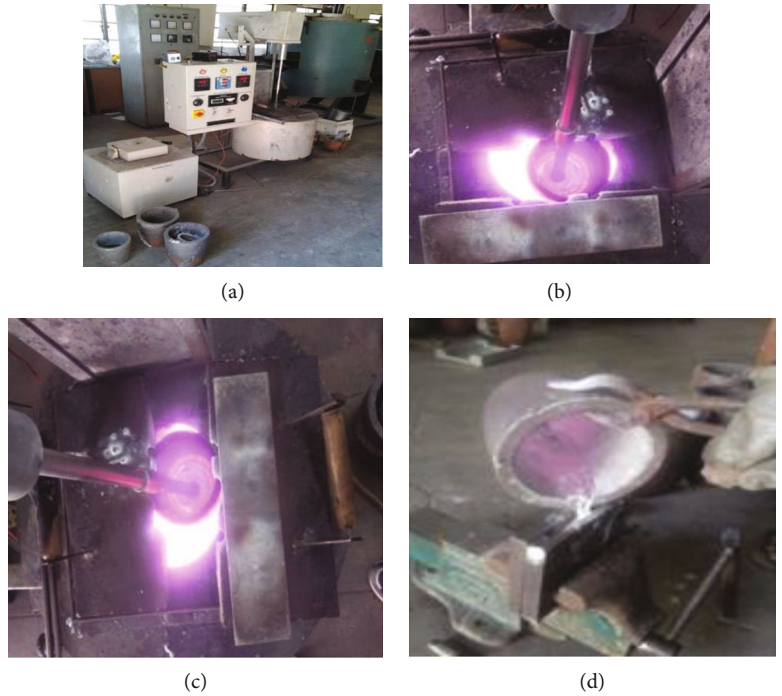

(a) (b)

(c) (d)

Figure 1: (a) Stir casting setup, (b) feeding of reinforcements, (c) stirring of composite slurry, and (d) pouring of the cast composite into dies.

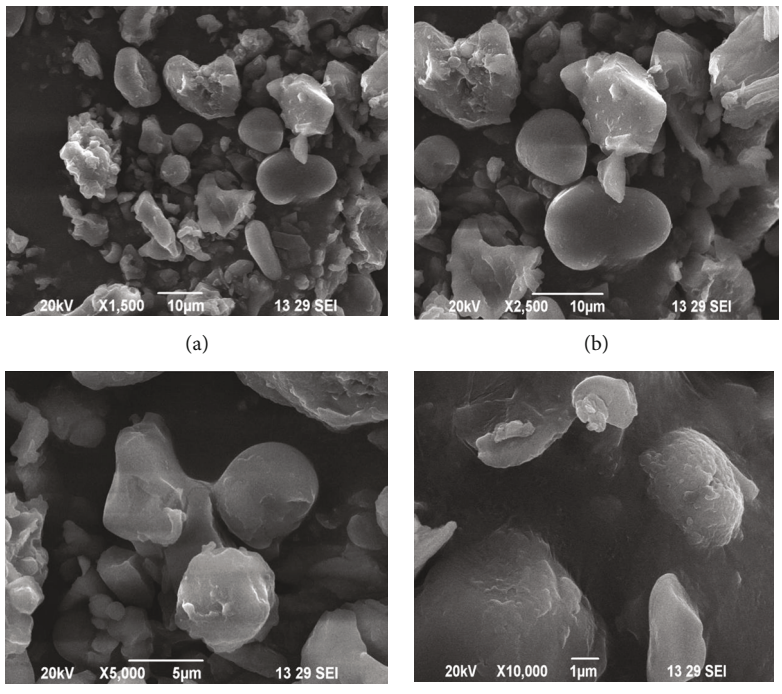

(a) (b)

(c) (d)

Figure 2: Microstructure illustration of (a)&(b) HBN and (c)&(d) CBN composites. The HBN particle size is ×1500 and ×2500 in 10 μm, and the CBN size is ×5000 in 5 μm and ×10000 in 1 μm as shown in Figures 2(a) and (d).

Figure 3: Wear testing arrangements in the pin-on-disc apparatus.

Table 1: Input parameters of wear testing and its additions..

Contribution factor	Level 1	Level 2	Level 3
HBN (%)	0.5	1.0	1.5
CBN (%)	1.0	2.0	3.0
Load (N)	10	30	50
Speed of sliding (m/s)	1	2	3
Distance of sliding (m)		2000	

The regression equation for this MMC's wear rate is provided by

$$\begin{aligned}\text{Wear rate} = {} & 0.63631 - (0.328127 * \%\text{HBN}) \\ & - (0.0451929 * \%\text{CBN}) + (0.00144872 * \text{load}) \\ & - (0.00146963 * \text{SS}) + (0.124477 * \%\text{HBN} * \%\text{HBN}) \\ & - (0.0018006 * \%\text{CBN} * \%\text{CBN}) - (1.68475e-006 * \text{load} * \text{load}) \\ & + (0.00661419 * \text{SS} * \text{SS}) + (0.0172865 * \%\text{HBN} * \%\text{CBN}) \\ & - (0.000837525 * \%\text{HBN} * \text{load}) - (0.0151258 * \%\text{HBN} * \text{SS}) \\ & - (0.000211329 * \%\text{CBN} * \text{load}) - (0.00844244 * \%\text{CBN} * \text{SS}) \\ & + (0.000395297 * \text{load} * \text{SS}),\end{aligned}$$

$$S = 0.0109344 \quad R - Sq = 99.23\% \quad R - Sq(\text{adj}) = 98.29\%. \tag{2}$$

Table 3 shows the percent contribution of input parameters for the wear rate using an analysis of variance (ANOVA) table.

4.1. Influence of Reinforcement Addition. The use of hexagonal boron nitride (self-lubricating) and cubic boron nitride in a soft and ductile matrix increases the hardness and hence reduces the wear rate of the matrix alloy, lowering the wear rate of composites. The dislocation density rises due to a thermal mismatch (difference in thermal expansion coefficient) among the matrix alloy and the reinforcements. Increased dislocation density improves the materials' resistance to plastic deformation and minimizes friction during sliding motion, minimizing crack propagation during wear. The Aluminum 94%, HBN 3%, and CBN 3% were used in reinforcement in this work. In the use of wt %, the wear resistance is verified by pin-on-disc.

Table 2: Observations of the wear test.

Expt. no	% HBN	% CBN	Load (N)	Slidingspeed (m/s)	Wear rate (mm^3/m)
1	0.5	1	10	1	0.4515
2	0.5	1	30	2	0.4966
3	0.5	1	50	3	0.5546
4	0.5	2	10	2	0.3936
5	0.5	2	30	3	0.4369
6	0.5	2	50	1	0.4416
7	0.5	3	10	3	0.3397
8	0.5	3	30	1	0.3445
9	0.5	3	50	2	0.3691
10	1	1	10	2	0.3437
11	1	1	30	3	0.3846
12	1	1	50	1	0.3798
13	1	2	10	3	0.2965
14	1	2	30	1	0.3161
15	1	2	50	2	0.3264
16	1	3	10	1	0.2699
17	1	3	30	2	0.2727
18	1	3	50	3	0.2833
19	1.5	1	10	3	0.3212
20	1.5	1	30	1	0.3223
21	1.5	1	50	2	0.3268
22	1.5	2	10	1	0.2773
23	1.5	2	30	2	0.2842
24	1.5	2	50	3	0.2979
25	1.5	3	10	2	0.2070
26	1.5	3	30	3	0.2059
27	1.5	3	50	1	0.2354

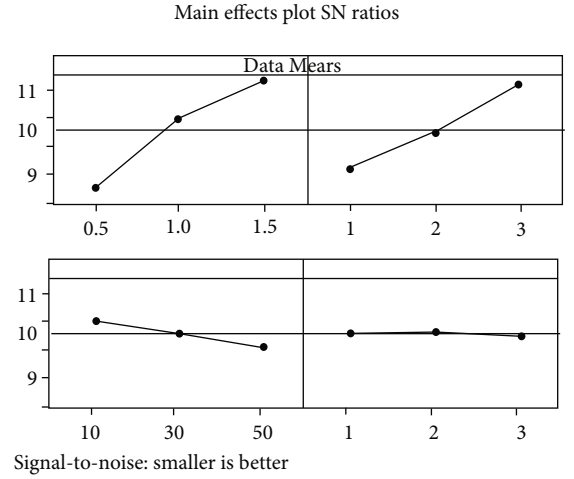

Figure 4: Key outcome plots of S/N ratios about the wear rate.

4.2. Influence of the Applied Load. Sliding wear is related to the applied force and the sliding distance and inversely proportional to the degraded surface's hardness. The shift in

Table 3: ANOVA observations of % contribution of inputs for the wear rate.

Source	DF	Seq SS	F	P	Contribution %
% HBN	1	0.10125	82.13400	0.00171	55.749
% CBN	1	0.06167	4.69300	0.05113	33.957
Load	1	0.00550	2.67300	0.12802	3.028
SS	1	0.00038	0.00500	0.94500	0.206
%HBN ∗ %HBN	1	0.00581	48.50900	0.00932	3.199
%CBN ∗ %CBN	1	0.00002	0.16200	0.69404	0.010
Load ∗ load	1	0.00000	0.02300	0.88262	0.002
SS∗SS	1	0.00026	2.19100	0.16456	0.144
%HBN ∗ %CBN	1	0.00135	7.01600	0.02122	0.744
%HBN ∗ load	1	0.00133	6.58800	0.02469	0.730
%HBN ∗ SS	1	0.00089	5.37900	0.03882	0.492
%CBN ∗ load	1	0.00020	1.67800	0.21958	0.111
%CBN ∗ SS	1	0.00082	6.85400	0.02247	0.452
Load ∗ SS	1	0.00070	5.81100	0.03287	0.383
Error	12	0.00144			0.791
Total	26	0.18161			100.00

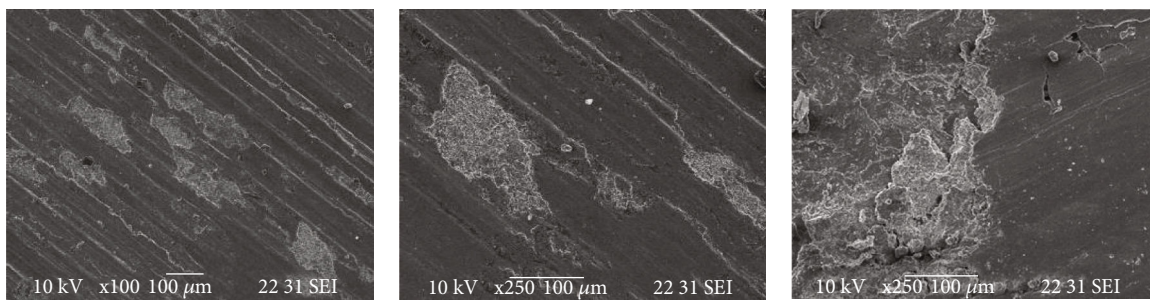

(a) (b) (c)

Figure 5: SEM image worn-out surface of experiments.

wear behavior with increasing load may be described using Archard's theory.

The observed increase in the wear rate was caused by the fact that as the applied stress rises, so does the permeation of stiff asperities of the counter exterior into the softer pin surface, as well as deformation and fracture of the softer surface asperities. As the load grows, thermal softening and plastic deformation tend to serve on the MMC. This might be due to the weight-bearing capacity of the reinforcements and base metal. As a result, at low speeds, the abrasive wear process takes over, in which the fracture strength exceeds the fracture strength, resulting in fracture owing to higher produced stresses. The material may be transported from the pin to the disc owing to the chafing action of broken reinforcing particles on the steel disc and the displacement of the matrix from the pin's surface. More energy is given as the load grows, and some of it is transformed to heat energy. The heating caused by friction increases as the applied load increases, resulting in localized adhesion of the pin surface to the counter surface as the interface temperature rises. As the load rises, so does the pin's penetration into the composite surface, resulting in a quicker rate of wear.

4.3. Consequences of Sliding Speed. The results show that when a combination of percent HBN addition, percent CBN addition, and applied load is used, the frictional heat created between the pin and the steel disc is influenced by sliding speed. Where the reinforcements are penetrated from the pin to the counter plate, the degree of softening and frictional heat are directly proportional to each other. However, increasing the sliding speed reduces the wear rate, which is caused by reinforcement pulling due to thermal mismatch. When the drawn reinforcing particles come into contact with the steel disc, the wear rate is reduced at greater speeds.

4.4. Wear Surface Morphology of Aluminum Metal Matrix Composites by SEM Analysis. An SEM was used to examine the worn-out surface of selected specimens after the wear

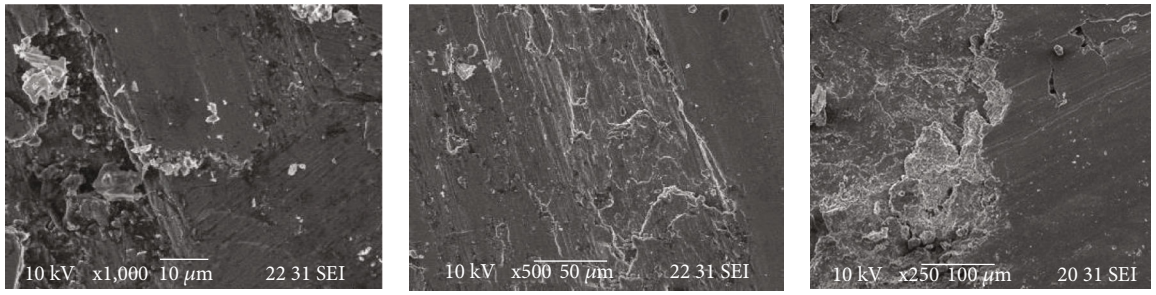

(a) (b) (c)

Figure 6: SEM image worn-out surface of experiments 2, 14, and 26.

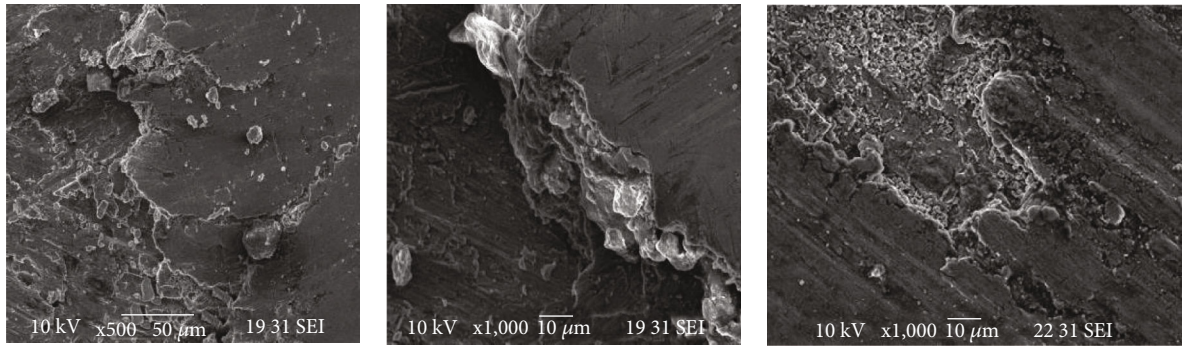

(a) (b) (c)

Figure 7: SEM image worn-out surface of experiments 9, 18, and 27.

test (SEM). Figures 5(a)–5(c) demonstrate the surface morphology of the hybrid composite for experiments 1, 4, and 7. It appears that cavities generated in the composite matrix have aligned parallel to the direction of sliding when tested at low load (10 N). During the scouring process, several particles particles were chopped off. In certain zones, the composite lattice has released smaller particles over the worn surface of the AA6061-HBN-CBN Hybrid composite. Deep and persistent grooves cause the oxide layer casting to fracture, resulting in increased wear loss. The two composites' worn surfaces had finer grooves and modest plastic distortion at the groove margins. The reinforcing also gives the surface a smooth appearance. Notably, fissures grow parallel to the sliding direction. When the applied load is low, the reinforcements fracture, fragment, or move along the crack lines. Although cavitations appear to be modest, deep cracks and grooves are plainly seen with increasing applied force.

SEM images for experimental conditions 2, 14, and 26 are depicted in Figures 6(a)–6(c). The worn surface changes appearance when subjected to 30 N of force. The cavitations are greater in this example than in the previous one. Some substructures run in the same direction as the sliding direction. The worn surface had resulted in subtle grooves and minor scratches. The ploughing effect of the counter disc's strong asperities and hardened worn detritus creates the grooves. Wear would be reduced if the tungsten carbide content was increased. The structures of worn surfaces change depending on the sliding speed and applied force. When

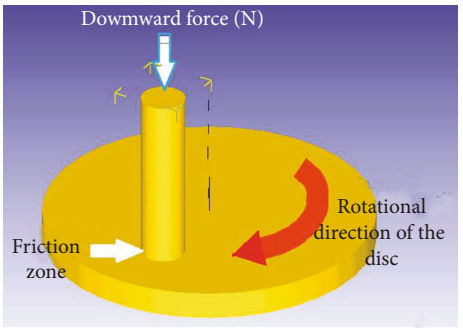

Figure 8: Modeling and assemblage of the pin-on-disc wear test in DEFORM 3D.

the sample is rubbed on a steel disc at a low sliding speed and applied force, the aluminum matrix appears to expand along the sliding direction. Cavitations have also increased. The hard particles seem to have fashioned a few holes (for example, HBN and CBN particulates)

Figures 7(a)–7(c) show SEM images for experimental conditions 9, 18, and 27. During sliding, hard particles dissolve the steel counter face, forming a thin coating of oxidized iron that acts as an ointment. Hard particles at grain boundaries would reduce particle breakage. Massive plastic strains in the composite network can cause subsurface breaks and delamination when in close contact with the steel counter face. Figure 7(a) depicts fractures occurring at

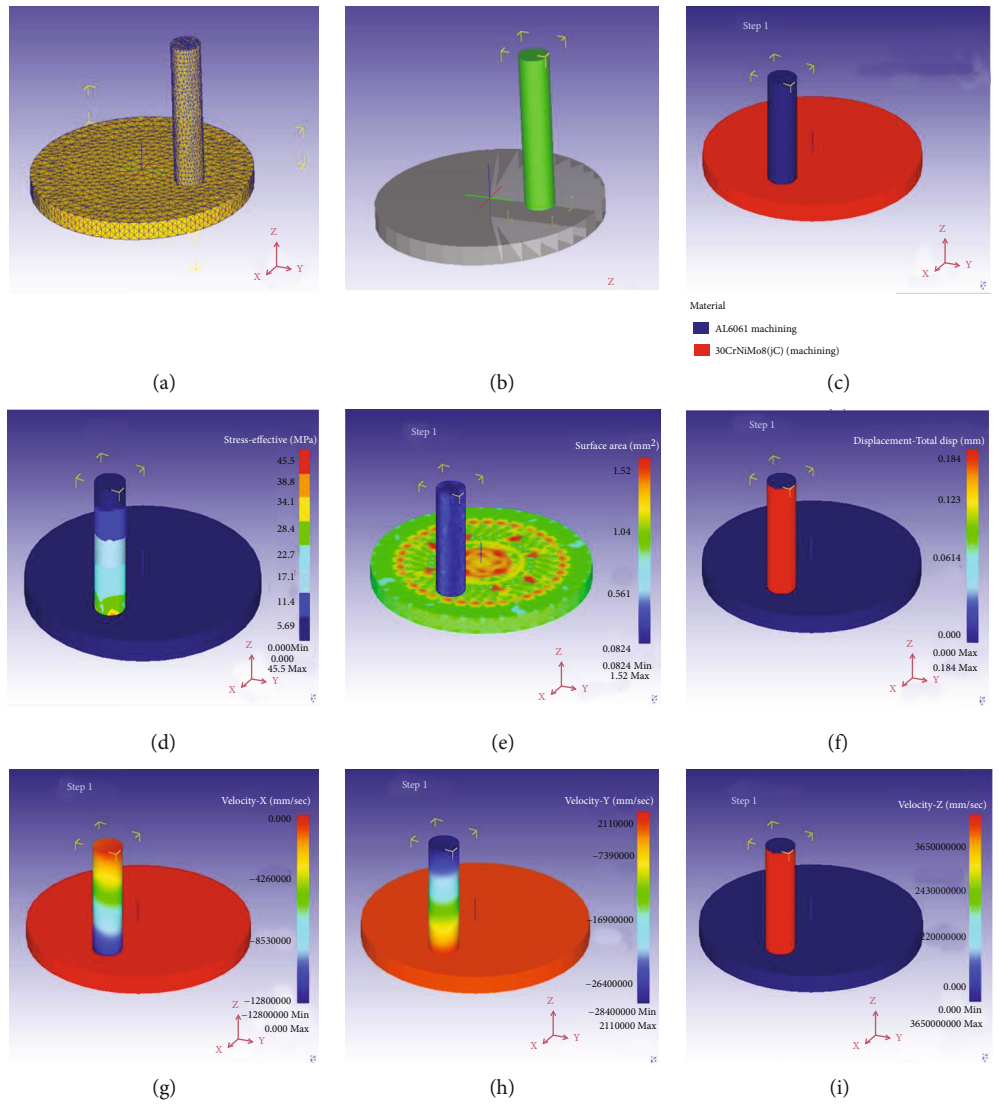

Figure 9: Simulation results of wear behavior.

aluminum grain boundaries as a result of strain hardening of aluminum during sliding with increasing stress and reinforcement explosion from aluminum grain boundaries as a result of increasing load. The wear rate reduces at 3 m/s, suggesting less material loss from the surface. Figure 7(c) shows a lot of grooves on the surface.

4.5. Validation of Wear Test through Simulation. The multidirectional simulation tool DEFORM 3D is used for all dynamically oriented analysis, especially used for the 3-dimensional analysis and simulation of all metal forming and machining techniques. We can easily predict the properties of all domain-related elements. As mentioned in the previous experimental stage, using the pin-on-disc apparatus, the friction level and the wear rates can be easily calculated by this simulation procedure. Based on this, the simulation procedures have been originated for the bid of comparing the stress, velocity, and displacement for the highlighted value which has been arrived from the experimental part. The clockwise rotation of the disc can be modelled and located in the simulation platform with the vertical placement of the pin model. For both the pin and disc models, the material attributes were picked from the materials library.

The boundary conditions have been specified based on its rotation about the rotating disc assembly's center axis; similarly, a vertical downward force of 50 N can be applied over the pin in the DEFORM 3D simulation tool's z-axis as shown in Figure 8. The DEFORM 3D platform can simulate the frictional contact in a wear test.

The convergence relative mesh size was preferred in this case, and it was applied to both the friction plate and the pin element's surface. Both are in their correct positions, as revealed in Figures 9(a) and 9(b), with physical contact between the pin and the disc. Figure 9(c) shows the material properties of Al6061 for the pin element and 30CrNiMo8 steel for the revolving disc, which are labelled with distinct colors. As illustrated in Figure 9(d), the von Mises or effective stress was achieved in one of the experimental steps between the pin and the rotating disc. Here, the tension is

largest at the contact surface due to the gradually imposed load; it decreases lower along the vertical z-axis in DEFORM 3D. Figure 9(e) depicts the frictional impact on a disc with a surface area of 1.52 mm^2. The dynamics simulation tool measured the displacement at 0.184 mm throughout the pin length. When there is a condition of friction between the mating surfaces, this approach can be utilized to anticipate stresses and displacements. Figures 9(g) and 9(h) and I demonstrate how the velocities on both the x-, y-, and z -axes can be anticipated in Figure 9(i). The y- and z-axis velocities are only active in this case. There was no velocity value obtained along the x-axis direction.

5. Conclusion

The addition of hexagonal boron nitride and cubic boron nitride improves the wear resistance of aluminum AA6061. Among these two, hexagonal boron nitride contributes more than its cubic structured counterpart. Wear resistance decreases as the load increases, independent of the composition, and mass loss increases. A thin tribo film is formed by the HBN reinforcements that have been removed. It keeps metal from coming into direct contact with the sliding surface, as well as CBN particles from fracturing. These reinforcements also serve as a barrier, inhibiting dislocation movement, which manifests as little patches. The greatest weight percent of HBN and CBN resulted in the least amount of material loss during wear. The deformation resistance given by CBN, which breaks into little pieces to produce wear debris particles, is a noteworthy component of this wear research. This garbage keeps the plate from penetrating the metal, securing the delicate aluminum structure and enhancing wear blockage. Affirmation experiments were communicated using the empirical equation. The discrepancy between the actual and expected readings was less than 5%. Better comparison has been created for the sake of prediction utilizing DEFORM 3D and can be taken as a future scope of work in the same operating conditions.

Data Availability

The data used to support the findings of this study are included in the article. Should further data or information be required, these are available from the corresponding author upon request.

Disclosure

This research was performed as part of the employment in Hawassa University, Ethiopia.

Conflicts of Interest

The authors declare that there are no conflicts of interest regarding the publication of this paper.

Acknowledgments

The authors appreciate the technical assistance to complete this experimental work from the department of mechanical engineering, Saveetha University, Chennai, Tamil Nadu, India.

References

[1] N. Natarajan, S. Vijayarangan, and I. Rajendran, "Wear behaviour of A356/25SiC_p aluminium matrix composites sliding against automobile friction material," *Wear*, vol. 261, no. 7-8, pp. 812–822, 2006.

[2] J. Singh, "Fabrication characteristics and tribological behaviour of Al/SiC/gr hybrid aluminum metal matrix composites: a review," *Friction*, vol. 4, pp. 1–17, 2016.

[3] J. M. Mistry and P. P. Gohli, "An overview of diversified reinforcement on aluminium metal matrix composites: tribological aspects," *Journal of Indian tribology*, vol. 231, pp. 399–421, 2016.

[4] A. E. Baradeswaran and A. E. Perumal, "Influence of B_4C on the tribological and mechanical properties of Al 7075-B_4C composites," *Composites Part B: Engineering*, vol. 54, pp. 146–152, 2013.

[5] K. R. Padmavathi and R. Ramakrishnan, "Tribological behaviour of aluminium hybrid metal matrix composite," *Procedia Engineering*, vol. 97, pp. 660–667, 2014.

[6] N. S. Prabhakar, N. Radhika, and R. Raghu, "Analysis of tribological behavior of aluminium/B_4C composite under dry sliding motion," *Procedia Engineering*, vol. 97, pp. 994–1003, 2014.

[7] N. S. Kumar, V. M. Ravindranath, and G. S. Shankar, "Mechanical and wear behaviour of aluminium metal matrix hybrid composites," *Procedia Materials Science*, vol. 5, pp. 908–917, 2014.

[8] P. Sharma, D. Khanduja, and S. Sharma, "Dry sliding wear investigation of Al6082/Gr metal matrix composites by response surface methodology," *Journal of Materials Research and Technology*, vol. 5, no. 1, pp. 29–36, 2016.

[9] A. R. Riahi and A. T. Alpas, "The role of tribo-layers on the sliding wear behavior of graphitic aluminum matrix composites," *Wear*, vol. 251, no. 1-12, pp. 1396–1407, 2001.

[10] P. Bindumadhavan, H. Wah, and O. Prabhakar, "Dual particle size (DPS) composites: effect on wear and mechanical properties of particulate metal matrix composites," *Wear*, vol. 248, no. 1-2, pp. 112–120, 2001.

[11] R. Praveenkumar, P. Periyasamy, V. Mohanavel, and M. M. Ravikumar, "Mechanical and tribological behavior of Mg-matrix composites manufactured by stir casting," *International Journal of Vehicle Structures and Systems*, vol. 11, pp. 117–120, 2019.

[12] P. Periyasamy, B. Mohan, and V. Balasubramanian, "Effect of heat input on mechanical and metallurgical properties of friction stir welded AA6061-10% SiCp MMCs," *Journal of Materials Engineering and Performance*, vol. 21, no. 11, pp. 2417–2428, 2012.

[13] R. Praveenkumar, P. Periyasamy, V. Mohanavel, and D. Chandramohan, "Microstructure and mechanical properties of mg/WC composites prepared by stir casting method," *International Journal of Mechanical Engineering and Technology (IJMET)*, vol. 9, no. 10, pp. 1504–1511, 2018.

[14] L. Natrayan and M. Senthil Kumar, "Optimization of wear parameters of aluminium hybrid metal matrix composites by squeeze casting using Taguchi and artificial neural network," in *Sustainable Manufacturing and Design*, vol. 10, pp. 223–234, Woodhead Publishing, 2021.

[15] L. Natrayan and M. Senthil Kumar, "Influence of silicon carbide on tribological behaviour of AA2024/Al2O3/SiC/Gr hybrid metal matrix squeeze cast composite using Taguchi technique," *Materials Research Express*, vol. 6, no. 12, article 1265f9, 2019.

[16] L. Natrayan, V. Sivaprakash, and M. S. Santhosh, "Mechanical, microstructure and wear behavior of the material AA6061 reinforced SiC with different leaf ashes using advanced stir casting method," *International Journal of Engineering and Advanced Technology*, vol. 8, pp. 366–371, 2018.